



**HAL**  
open science

## A notched dielectric resonator antenna unit-cell for 60GHz passive repeater with endfire radiation

Duo Wang, Raphaël Gillard, Renaud Loison

► **To cite this version:**

Duo Wang, Raphaël Gillard, Renaud Loison. A notched dielectric resonator antenna unit-cell for 60GHz passive repeater with endfire radiation. The European Conference of Antennas and Propagation (EuCAP 2015), Apr 2014, The Hague, Netherlands. 10.1109/EuCAP.2014.6902500 . hal-01109895

**HAL Id: hal-01109895**

**<https://hal.science/hal-01109895>**

Submitted on 28 Jan 2015

**HAL** is a multi-disciplinary open access archive for the deposit and dissemination of scientific research documents, whether they are published or not. The documents may come from teaching and research institutions in France or abroad, or from public or private research centers.

L'archive ouverte pluridisciplinaire **HAL**, est destinée au dépôt et à la diffusion de documents scientifiques de niveau recherche, publiés ou non, émanant des établissements d'enseignement et de recherche français ou étrangers, des laboratoires publics ou privés.

# A Notched Dielectric Resonator Antenna Unit-Cell for 60GHz Passive Repeater with Endfire Radiation

Duo WANG, Raphaël GILLARD, Renaud LOISON

European University of Brittany: Institute of Electronics and Telecommunications of Rennes, INSA, UMR CNRS 6164, 35708 Rennes, France, {duo.wang, raphael.gillard, Renaud.loison}@insa-rennes.fr

**Abstract**—This paper presents the preliminary design of a 60GHz passive repeater endfire array with dielectric resonator antenna (DRA) elements. The proposed DRA element utilizes simple notches at opposite corners of a square DRA to obtain polarization-conversion. By combining two DRA with notches on opposite diagonals, endfire radiation can be obtained. A 6x1 linear array is optimized and simulated as an initial demonstration.

**Index Terms**—60GHz, passive repeater, endfire array, notched dielectric resonator antenna.

## I. INTRODUCTION

Endfire antenna arrays play an important role in communication and radar [1] but their design meets many challenges. For example, microstrip patch arrays with ground plane do not easily provide endfire radiation due to the cancellation effect resulting from mirror image currents. Solutions using artificial magnetic conductors (AMC) or high impedance surfaces (HIS) [2] can address this issue but result in a quite complicated design and usually exhibit a reduced bandwidth. In this paper, we focus on the even more complex problem of planar reflecting surfaces with endfire radiation. The desired surface has to comply with two constraints: firstly, it must provide a full reflection of the incident wave (thus requiring a ground plane); and, secondly, it must produce a radiation parallel to the reflecting surface. Such a configuration may be encountered in passive repeaters [3] for indoor communications at 60 GHz, especially in the case of L- or T-shaped corridors [7]. Indeed, typical passive repeaters are of great attraction for their easy deployment, simple design and cost effectiveness.

In this paper, we propose to solve this problem by means of a reflector made of DRAs. One DRA in fundamental mode radiates like a magnetic dipole and can thus be backed by a ground plane [4-6]. Moreover, DRAs are particularly well suited for millimeter waves due to their intrinsic low loss [5], and they naturally exhibit a quite large bandwidth.

In [7], we demonstrated the possibility to obtain promising performance by loading consecutive square DRA with two different stub lengths coupled through slots in the ground plane. In the present paper, we propose a more simple solution requiring neither slot nor stub. The desired 180° phase shift between consecutive DRA is directly obtained thanks to notches in the dielectric material.

In section II, the modal analysis of a single notched DRA is carried out in order to obtain reflection with polarization conversion. Then, 2 DRAs with notches on opposite diagonals are combined to excite an orthogonal mode whose field configuration is compatible with endfire radiation. Finally, in section III, a preliminary 6x1 array is designed that reflects a large amount of power at endfire.

## II. DESIGN OF DRA CELL

### A. General Antenna Configuration

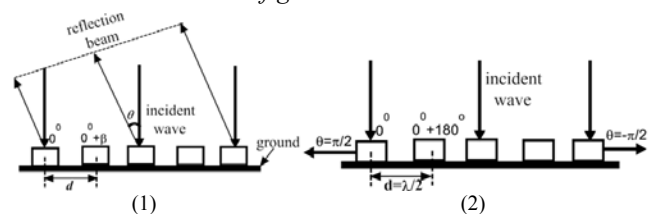


Fig. 1. (1) General working principle for passive repeater array based on DRA, (2) Proposed implementation for combined endfire/backfire radiation

Fig. 1 illustrates the typical foreseen configuration where DRA elements are regularly disposed over a ground plane and illuminated by an impinging plane wave under normal incidence. It is assumed this wave is produced by a remote source and the aim of the DRA reflector is to re-direct it at both endfire and backfire, as shown in [7]. Endfire and backfire radiation ( $\theta = \pm \pi/2$ ) can be achieved with out-of-phase elements by using a half wavelength inter-element spacing ( $d = \lambda/2$ ).

### B. Notched DRA element design

In this paper, the required 180° phase shift between consecutive DRA is obtained using a principle similar to the one used in [8] for 1-bit reflectarrays. Firstly, the incident linearly polarized wave is reflected in the orthogonal polarization by diagonally loading the radiating element. Secondly, consecutive elements exhibit loadings on opposite diagonals so that their respective reflections are out of phase. In this paper, the chosen element is a square DRA ( $L = 1.5\text{mm}$ ,  $\epsilon_r = 10$ , loss tangent = 0.002, and  $h = 1.35\text{mm}$ ) with square notches (Fig. 2) at corners. The DRA is backed by a ground plane.

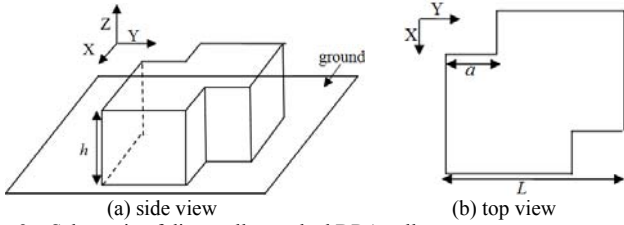


Fig. 2. Schematic of diagonally notched DRA cell

The notched size  $a$  is optimized to achieve polarization conversion when reflection occurs. The simulation is realized with Ansoft HFSS 13.0 assuming local periodicity and normal incidence.

Fig. 3 presents the scattering parameters of the cell when  $a=0.6\text{mm}$ .  $S_{11}$  measures the reflection on polarization  $y$  for a  $y$ -polarized incident wave ( $TE_{00}$  Floquet mode) while  $S_{21}$  measures the reflection on polarization  $x$  ( $TM_{00}$  Floquet mode).

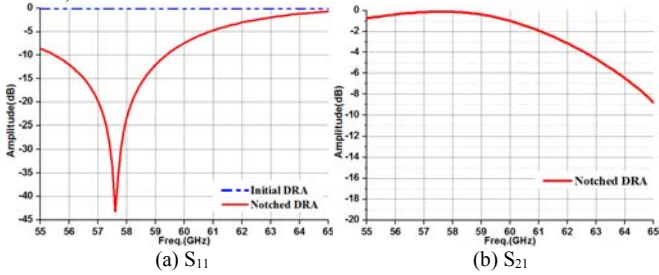


Fig. 3. S parameters for notched DRA when  $a=0.6\text{mm}$

The notched DRA cell obtains almost 100% polar-conversion at  $57.6\text{GHz}$  ( $S_{11}=-43\text{dB}$  and  $S_{21}=-0.2\text{dB}$ ), leaving a small margin from  $60\text{GHz}$ . S parameters of this initial DRA are also given in Fig.3 for comparison (as  $S_{21}<-50\text{dB}$ , it is omitted in Fig.3 (b)), which of course demonstrates a full reflection with no polar-conversion at all.

In order to go further, two DRAs with notches on opposite diagonals are now combined with a  $\lambda_0/2$  element-spacing ( $S=2.5\text{mm}$ ) as shown in Fig. 4. They are simulated again assuming local periodicity (the  $2\times 1$  unit-cell is now the combination of both DRAs) and normal incidence.

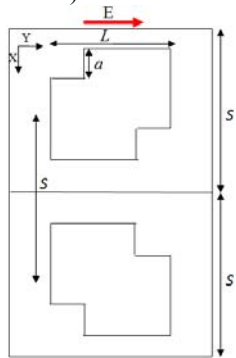


Fig. 4. Schematic for  $2\times 1$  unit-cell with opposite-notched DRA

Fig. 5 shows the field snapshots for a  $y$ -polarized incident wave ( $TE_{00}$  excitation). As can be seen, the best mode conversion is obtained at  $61.2\text{GHz}$ . This frequency shift may be explained by the differences in the coupling mechanisms

(as one DRA is not surrounded anymore by identical neighbors).

At this frequency, the E-field distribution on two opposite-notched DRA shows opposite  $E_x$  components but identical  $E_y$  components. Since the  $x$ -spacing is  $\lambda_0/2$ ,  $E_x$  components on the two cells would produce strong superposition at endfire ( $\theta=\pm\pi/2$  for  $\phi=0$  or  $\pi$ ), as desired. On the other hand, the  $E_y$  components will be responsible for the residual broadside radiation with  $y$ -polarization (same as the incident wave).

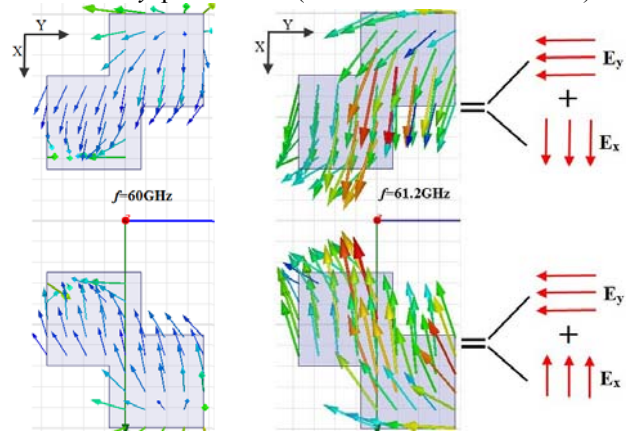


Fig. 5. E-field distribution for  $2\times 1$  unit-cell around  $60\text{GHz}$

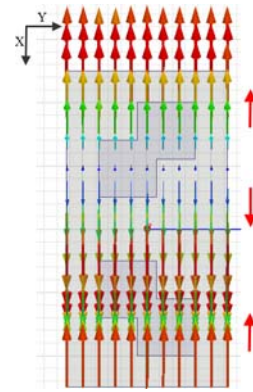


Fig. 6. E-field distribution of  $TM_{10}$  mode for incident wave

Regarding Floquet analysis, endfire radiation (with polarization conversion) is obtained when power is reflected back on the  $TM_{10}$  mode (see corresponding field snapshot in Figure 6). Then, Figure 7 presents the scattering parameters of the 2-DRA unit-cell. As before,  $S_{11}$  measures the power that is reflected on the incident  $TE_{00}$  mode, and  $S_{51}$  measures the polar-conversion to  $TM_{10}$  mode.

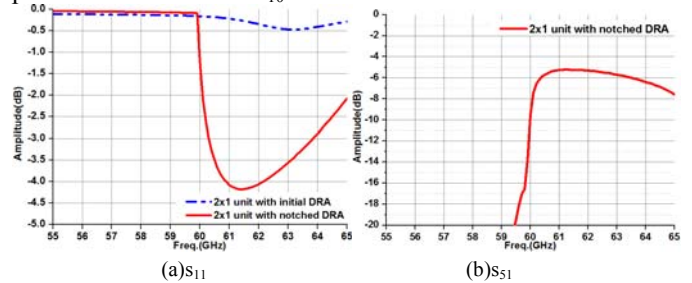


Fig. 7. S parameters for  $2\times 1$  unit-cell

As these results confirm, the maximum polar-conversion is obtained at 61.2GHz ( $S_{11}=-4.2\text{dB}$  and  $S_{51}=-5\text{dB}$ ). As comparison, the 2x1 unit-cell with initial DRA still demonstrates strong reflection (its  $S_{51}<-40\text{dB}$  is not included in Fig. 7(b)).

### III. 6X1 ARRAY IMPLEMENTATION AND OPTIMIZATION

In this section, a preliminary 1-D linear array with 6 elements is considered, as shown in Fig. 8. Following the initial modal analysis of the previous section, the objective is now to optimize the radiation performance itself. The main parameter, namely the notch size  $a$  on each DRA, is used to maximize polarization conversion at endfire. Since the mutual coupling effects on the elements are restricted symmetrically along  $x$ -axis, following discussion only considers the top half DRAs, marked as DRA\_1, DRA\_2 and DRA\_3, with corresponding notched sizes  $a_1$ ,  $a_2$  and  $a_3$ .

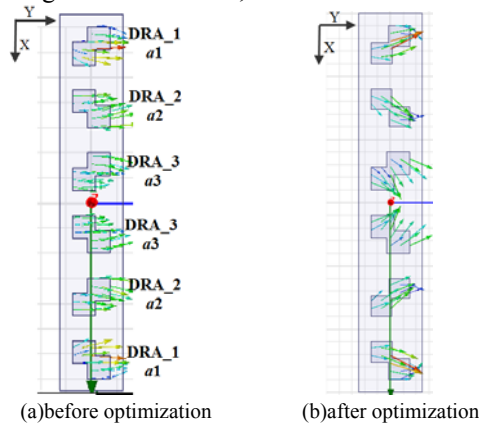


Fig. 8. E-field distribution for 6x1 array at 60GHz

The optimized function measures the amount of reflection at broadside relatively to the amount of reflection at endfire. It is given as:

$$\Gamma = \frac{|E_{\phi}(\text{broadside})|}{|E_{\phi}(\text{endfire})|} = \frac{|E_{\phi}(\varphi = 0, \theta = 0)|}{|E_{\phi}(\varphi = 0, \theta = \pm 90^{\circ})|} \quad (1)$$

for a  $y$ -polarized wave under normal incidence. Logically, as we seek for minimum reflection at broadside and maximum endfire radiation, the smallest  $\Gamma$  would be our final optimization goal. In Fig. 9, an example is given to show how  $\Gamma$  helps to locate the optimal  $a_1$ .

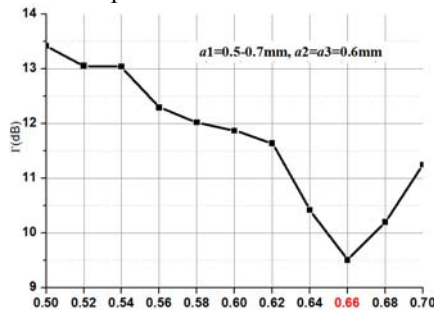


Fig. 9.  $\Gamma$  optimization of  $a_1$

The final optimization result for the 6x1 array is determined as  $a_1=0.66\text{mm}$ ,  $a_2=0.7\text{mm}$  and  $a_3=0.6\text{mm}$ . This leads to  $\Gamma=3.47\text{dB}$  and the corresponding E-field distribution is also given out in Fig.8 (b). For comparison, its performance is sketched in Fig. 10 with that of the initial array (i.e.  $a_1=a_2=a_3=0.6\text{mm}$  as derived in section II) before optimization.

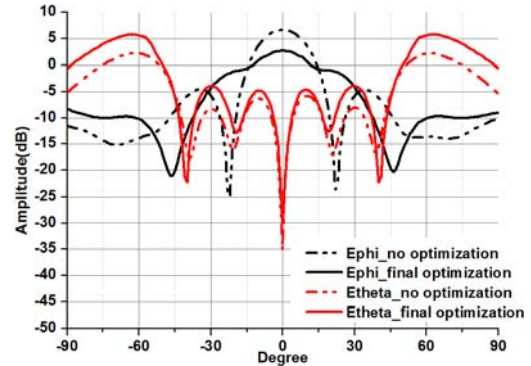


Fig. 10. E pattern comparison of initial dimension and final optimization( $\phi=0$  plane)

As can be seen, the reflection at broadside has been reduced from 6.68 dB to 2.84 dB. In the meantime, the radiation at endfire has risen from -5.19 dB to -0.63 dB. Although the maximum radiation is not obtained at endfire but at  $\pm 65^{\circ}$ , a large amount of the reflected power is now redirected longitudinally.

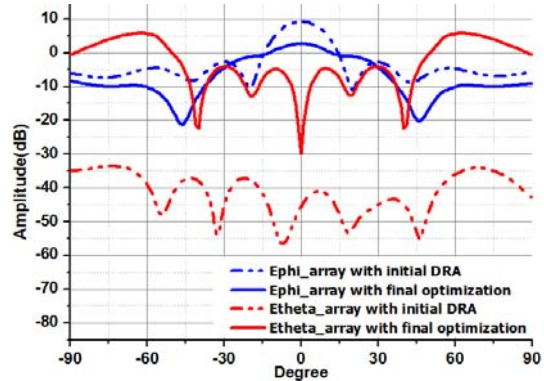


Fig. 11. Comparison of array with notched DRAs after final optimization and array with non-notch DRAs

In Fig. 11, the optimized 6x1 array is also compared to a similar array with the initial DRAs ( $L=1.5\text{mm}$ ,  $h=1.35\text{mm}$ ,  $a=0$ ). This clearly demonstrates that a strong polar-conversion has been achieved thanks to the used DRA reflector. This also shows that most of the power is now directed close to endfire.

### IV. CONCLUSION

This paper proposes a simple structure using notched DRA cells as a preliminary step towards a passive repeater array with endfire radiation. Based on the principle of polar-conversion, this structure transforms a normally incident plane wave into radiation close to endfire. The interest of the concept and an associated design methodology has been

validated in simulation for a quite simple 6x1 array demonstrator. Further steps are now required to provide results for a larger antenna and to perform an experimental validation.

#### REFERENCES

- [1] R. W. P. King, and S. S. Sandler, "The Theory of Endfire Arrays," *IEEE Transaction on Antennas and Propagation*, vol. 12, pages: 276-280, 1964
- [2] G. S. Reddy and Z. C. Alex, "Extended Dipole Antenna with AMC Spiral Ground and Via Holes for Millimeter Wave Application," *Progress In Electromagnetics Research Symposium Proceedings*, September, 2011.
- [3] Y. Huang, N. Yi, Z. Xu, "Investigation of using passive repeaters for indoor radio coverage improvement," *IEEE Antennas and Propagation Society International Symposium*, vol. 2, no. 12, pp. 1623-1626, 2004.
- [4] R. K. Mongia, and A. Ittipiboon, "Theoretical and Experimental Investigations on Rectangular Dielectric Resonator Antennas," *IEEE Transaction on Antennas and Propagation*, vol. 45, no. 9, September, 1997.
- [5] R. K. Mongia, and P. Bhartia, "Dielectric resonator antennas—a review and general design relations for resonant frequency and bandwidth," *International Journal of Microwave and Millimeter-Wave Computer-Aided Engineering*, vol. 4, issue 3, pp. 230-247, July 1994
- [6] W. M. Abdel Wahab, D. Busuioc, and S. Safavi-Naeini, "Low Cost Planar Waveguide Technology-Based Dielectric Resonator Antenna (DRA) for Millimeter-Wave Applications: Analysis, Design, and Fabrication," *IEEE Transaction on Antennas and Propagation*, vol. 58, no. 8, August, 2010.
- [7] D. WANG, R. GILLARD, R. LOISON, "A 60GHz Passive Repeater with Endfire Radiation Using Dielectric Resonator Antennas," accepted by *IEEE Radio Wireless Week Symposium*, 2014.
- [8] S. Montori, L. Marcaccioli, R.V. Gatti, "Constant-Phase Dual Polarization MEMS-Based Elementary Cell for Electronic Steerable Reflectarrays," *Microwave Conference, EuMC2009*, pp. 33-36, 2009.